Detailed Investigation of Causes of Image Degradation in A Large Area Liquid Crystal Lens with Concentric Electrodes

Amit Bhowmick[2,3], Liwei Li [2,3], Afsoon Jamali[4], Doug Bryant[3], Sandro Pintz[4] and Philip Bos[1,2,3]

pbos@kent.edu
[1]Physics Dept, Kent State University
[2]Materials Science Graduate Program , Kent State University
[3]Advanced Materials and Liquid crystal institute, Kent State University, Kent, OH 44240, USA
[4]Meta Reality Labs
Keywords: Liquid Crystal, Lens

ABSTRACT

Liquid crystal based lenses with concentric electrodes are needed for applications where high optical quality is required. To achieve that quality , the sources of performance degradation and methods to overcome them are presented.

1. Introduction

Several papers have been written that describe the basics of the performance of liquid crystal based lenses. [1-8] However, a review of all factors of LC lens design and their contributions to the final performance have not been fully reviewed. In this paper, therefore, we start by introducing the LC simulations and lens modeling methods used, introduce main electro-optic lens design factors, and analytically and quantitatively analyze their effects on the lens performance in terms of particular metrics.

The basic design of the lens approach discussed in this paper is shown in Figure 1. for a small diameter lens. The design consists of concentric ITO electrodes that are interconnected with resistors to minimize the number of external driving voltages supplied by bus lines .

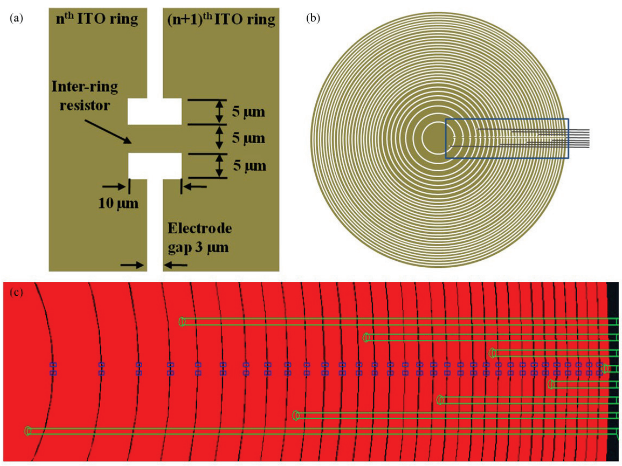

Figure 1. (a) Inter-ring resistor design; (b) Lens design diagram showing relative locations of resistors and bus lines; (c) Close-up at enclosed area.

2. LC Lens evaluation metrics.

Ideally, a collimated light beam parallel to the optical axis with plane wave is focused by a perfectly aspheric positive lens to form the airy disk pattern, containing most of the light intensity in the center lobe at the focal plane. Therefore, by comparing the intensity peak for LC lens to the ideal lens (same power) case (i.e. strehl ratio), its focusing ability can be determined, from which its imaging performance can be predicted as well. Thus, strehl ratio is the first primary metric to evaluate the quality of the LC lens.

The second metric used in this paper is Modulation Transfer Function (MTF), which is one of the most important specs for lens evaluation. The MTF curve shows the spatial frequencies of the image, and their corresponding contrast ratio, intrinsically determined by the lens. For example, with low frequencies, images can be well resolved with high contrast, and beyond the cutoff frequency, the images are blurred. Generally speaking, therefore, MTF demonstrates the relationship of lens resolution and image contrast.

3. LC calculations and lens modeling

The LC director field calculation takes the electrode pattern, applied voltages, cell thickness, and the liquid crystal properties as input, numerically calculates the 2D director profile throughout the cell. Then, the Optical Path Difference (OPD) or phase profile of the lens can be calculated by integrating the effective refractive index across the cell thickness for each point on the lens surface [3].

With a given lens OPD calculated, the light distribution at the focal plane is calculated using the Rayleigh-Sommerfeld diffraction equation. [9-10]

4. LC Lens Design factors

4.1 Phase steps

Analytically, given the diameter and focal length, the ideal parabolic phase profile for a positive lens across its aperture can be obtained:

$$OPD(r) \approx -\frac{r^2}{2f} \qquad (1)$$

Here, r is the lens radius, and f is the desired focal length. Outwards from the center, the width of each electrode is determined by its phase step within each electrode region being equally small as a fraction of λ (Green light λ = 543.5 nm), which tends to minimize quantization phase aberration caused by the discrete nature of electrode patterns [11]. In principle, the diffraction efficiency is proportional to the number of phase steps per wavelength of the light:

$$\eta \propto \left(\sin(\pi/q)/(\pi/q)\right)^2 \qquad (2)$$

Here, q is the number of steps per wavelength. In addition, this expression assumes no smoothness between adjacent stair steps.

Numerically, we can discretize the ideal continuous parabolic OPD to different phase steps per wave, and simulate the strehl ratio (Table.1). It's considered here that more than 8 phase steps/wave is required for acceptable lens performance.

	6 steps/wave	8 steps/wave	10 steps/wave
Analytical efficiency	91%	95%	97%
Numerical strehl ratio	93%	97%	98%

Table 1. Analytical diffraction efficiency and numerically calculated strehl ratio for different phase sampling rate

4.2 Gaps between electrodes

Gaps are needed to separate the electrodes in order to apply different voltages on different electrodes and tune the LC lens refractive power. In order to minimize the index aberration within the interstitial space, the gap between electrodes should be small, compared to thickness of the cell [12]. Both analytically and numerically, we analyze the lens efficiency for different electrode gap widths with the following example of a lens with diameter of 2.4mm, focal length of 400mm, 10 phase steps/wave, and 33 ring electrodes.

Analytically, the diffraction efficiency for different gap widths can be expressed as:

$$\eta \propto \left(1-\frac{\Lambda_F}{\Lambda}\right)^2$$

(3)

Here, Λ is the total width of the lens (diameter); Λ_F is the width of electrode gap areas (sum of gaps along diameter). Furthermore, in this expression, it assumes the gap areas are completely bad without phase smoothness between adjacent phase steps, and contribute nothing to the efficiency.
Numerically, we can determine the location and width of electrodes by assuming 10 phase steps/wave. With different gap width and perfect voltage profile, we can calculate the electric field distribution, LC 2D director profile, and LC lens OPD, which can be used to calculate the strehl ratio compared to the ideal lens for different gap widths. In addition, as the fringing field exists, the phase is smoother than the analytical case in the gap areas, therefore, a better efficiency is expected.

From the calculation results, it is found that the strehl ratio drops significantly as the gap width increases to 3 or 4μm (Table.2

	1μm gap	2μm gap	3μm gap	4μm gap
Analytical efficiency	94.6%	89.3%	84.2%	79.2%
Numerical strehl ratio	97.8%	93%	86.5%	81.5%

Table 2. Analytical diffraction efficiency and numerically calculated strehl ratio for different gap widths

In this example, the calculated MTF of LC lens with electrode gaps demonstrates a sharp contrast drop at low frequencies representing the uniformly scattered light. The cutoff frequency of LC lens is the same as ideal lens representing the same focusing ability as well (Fig. 2).

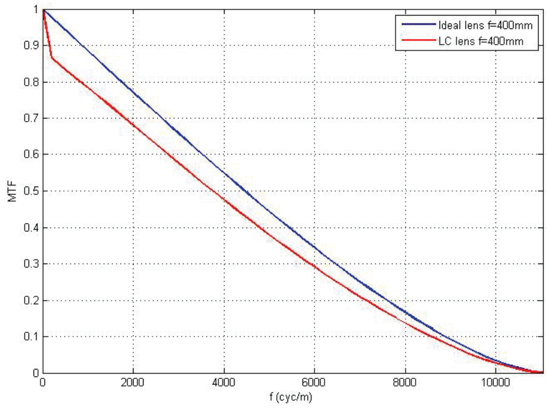

Figure 2. Calculated MTF for LC lens of 10 phase steps/wave, 3.5μm gaps

4.3 Floating electrodes and the effect of associated fringe fields.

To control the effect of haze associated with the electrode gaps, "floating electrodes" can be fabricated that cover the gaps in the driven electrodes . The modified device is shown in figure 3 :

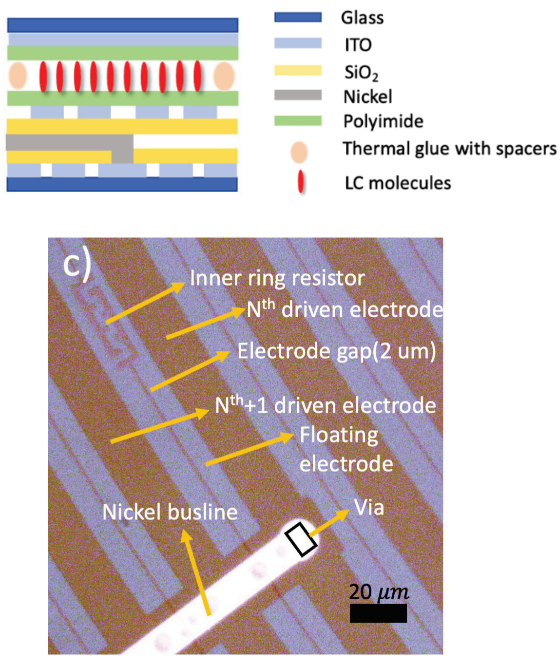

Figure 3 a) side view for the structure of the LC lens with 'floating' electrodes. In the picture the lower set of light blue electrodes viewed end on are the driven electrodes, and the upper set of light blue electrodes viewed end on are the floating electrodes. b) Microscope picture of the structure of the lens. The color is shown to add to the visualization of the structure. The driven and floating electrodes are transparent.

The effect of adding the floating electrodes is to significantly reduce the haze, with the resulting MFT curve being close to the ideal lens performance in figure 2.

While the floating electrodes provide substantially reduced haze, they create a smaller second source of haze. As shown in figure 4 below, there is a phase variation at the edges of the floating electrodes caused by a fringing electric field due to the potential difference of the floating electrodes and the underlying driven electrodes. We have found this cause of phase distortion can be eliminated through the addition of the thick insulator over the top of the floating electrodes. (not shown in figure 3)

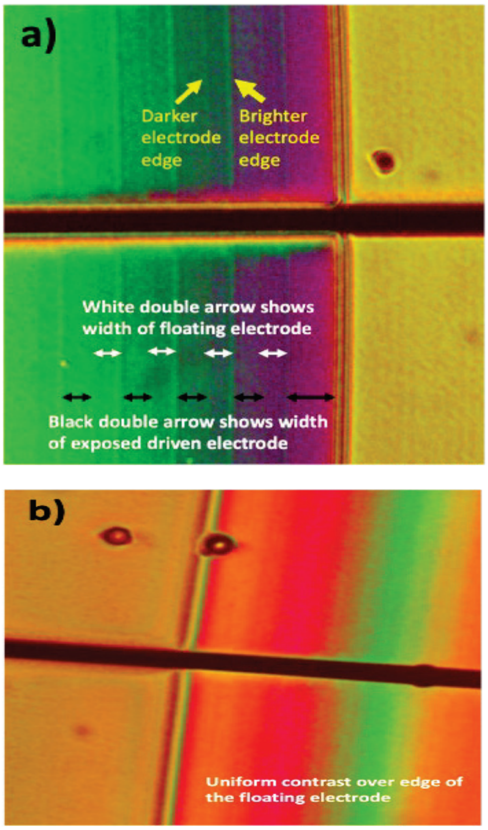

Fig. 4: Retardation change pictures resulting in a color change of the built cells under cross polarizer. a) before the addition of a thick insulator over the top of the floating electrodes . White and black double arrows are representing floating electrodes and exposed part of driven electrodes, respectively. Yellow single arrow sign is indicating the dark and bright edge of the floating electrodes. b) Picture showing smooth phase variation after addition of insulator layer .

4.4 The effect of phase resets

If a large diameter lens is required, the OPD given in equation 1 can be large, and for the case of a continuous phase profile result in a liquid crystal device thickness that causes the response time to be unacceptable. To solve that problem, phase resets can be used where the phase discontinuity is ideally an integer multiple of the wavelength of light. A section of a lens showing two phase discontinuities of 7 waves is shown in figure 5. Also shown in figure 5 is the distorted director profile at the phase discontinuity.

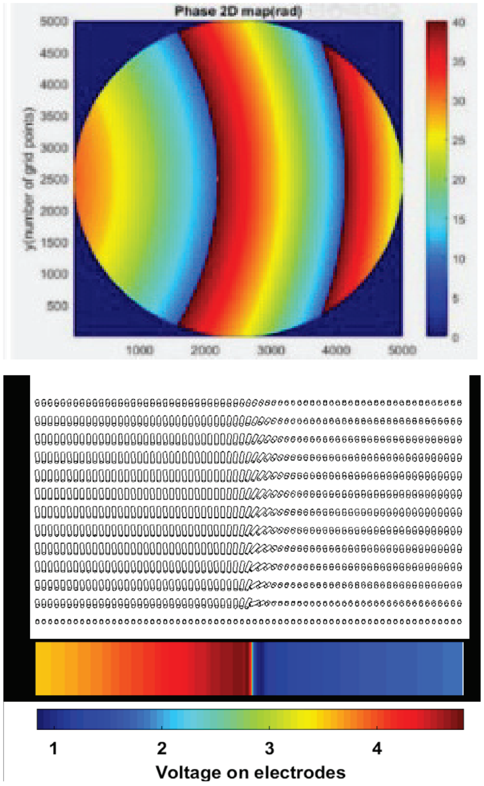

Figure 5. (top) A section of an example lens showing a segmented phase profile. The color scale is radians . (bottom) Director profile in the region of the phase discontinuity.

The distorted director field , causes light to be directed away from the desired deflection direction as shown in figure 6. The light scattered by this distortion is a source of haze that is undesirable, and can be minimzed by placing a light blocking layer over the region of phase distortion. Figure 7 shows a microscope picture that shows the region of phase distortion, and with a "black matrix" light blocking layer

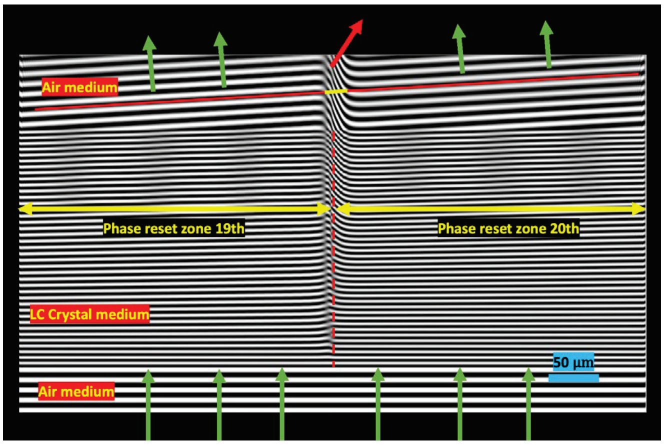

Figure 6. and FDTD picture showing the wavefront of light incident to a lens region that contains a phase reset at the bottom of the figure and exiting at the top. The red arrow shows the propagating of direction of light from the region of discontinuity.

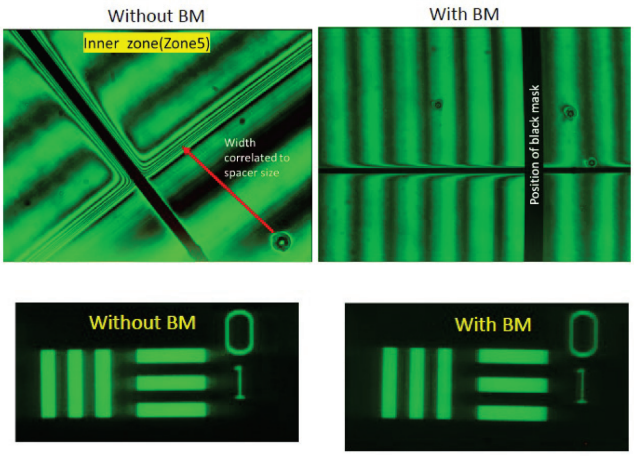

Figure 7. (top) shows microscope pictures of the phase distortion at a phase reset and the extent of the light blocking layer over that region. (bottom) shows the images of a resolution chart taken though lenses with and without the light blocking layer present.

Also shown in figure 7 is a picture taken though an example lens showing the reduction in haze that can result from the addition of the light blocking layer.

8. Conclusions

We have systematically studied the effects of different design factors on liquid crystal based electro-optic lens performance with modeling, and have shown approaches toward mitigating image degradation.

9. References

[1] H. K. Hong, et al., "Electric-Field-driven LC lens for 3-D/2-D autostereoscopic display," *J. Soc. Info. Display* Vol.17, pp.399-406, (2009).

[2]T. Shibata, T. Kawai, K. Ohta, M. Otsuki, N. Miyake, Y. Yoshihara, T. Iwasaki, "Stereoscopic 3D display with optical correction for the reduction of the discrepancy between accommodation and convergence," Journal of the SID, 13(8), 665-671 (2005).

[3] Liwei Li, Lei Shi, Doug Bryant, Tony Van Heugten, Dwight Duston, Philip J. Bos, 'Design and modeling of a refractive liquid crystal lens for tunable optical correction in 3-D stereoscopic displays', SID Symposium Digest, volume 42, Issue 1, pp. 9-12 (2011).

[4] G Li, DL Mathine, P Valley, P Äyräs, JN Haddock, et al, "Switchable electro-optic diffractive lens with high efficiency for ophthalmic applications," Proceedings of the National Academy of Sciences, 103, 16, 6100-6104 (2006).

[5] Mao Ye, Susumu, Sato, "Liquid crystal lens with focus movable along and off axis," Optics Communications, 4-6, 225, 277-280 (2003).

[6] Hongwen Ren, David W. Fox, Benjamin Wu, and Shin-Tson Wu, "Liquid crystal lens with large focal length tunability and low operating voltage," Optics Express, Vol. 15, No. 18 (2007).

[7] Tigran Galstian, Vladimir Presniakov, Karen Asatryan, "Method and apparatus for spatially modulated electric field generation and electro-optical tuning using liquid crystals", US patent 0229754 (2007).

[8] Tigran Galstian, Vladimir Presniakov, Karen Asatryan, Amir Tork, "Electricallly variable focus polymer-stabilized liquid crystal lens having non-homogenous polymerization of a nematic liquid crystal/monomer mixture", US patent 7667818 (2010).

[9] Joseph W. Goodman, Introduction to Fourier Optics, McGraw-Hill, second edition, (1988).

[10] David Voelz, Computational Fourier Optics – A matlab tutorial, Tutorial texts, SPIE, (2011).

[11] Stern, M.B, "Binary optics fabrication" in Micro-optics: Elements, Systems and Applications, (H.P.Herzig,Taylor&Francis, London, 1997).

[12] P. F. Brinkley, S. T. Kowel, C.H. Chu, "Liquid crystal adaptive lens: beam translation and field meshing," Applied Optics,27,4578-4586 (1988).